

# Condensation energy and spectral functions in high-temperature superconductors

M. R. Norman

*Materials Sciences Division, Argonne National Laboratory, Argonne, Illinois 60439*

M. Randeria

*Tata Institute of Fundamental Research, 400005 Mumbai, India*

B. Jankó

*Materials Sciences Division, Argonne National Laboratory, Argonne, Illinois 60439*

J. C. Campuzano

*Materials Sciences Division, Argonne National Laboratory, Argonne, Illinois 60439  
and Department of Physics, University of Illinois at Chicago, Chicago, Illinois 60607*

(Received 3 December 1999)

If high-temperature cuprate superconductivity is due to electronic correlations, then the energy difference between the normal and superconducting states can be expressed in terms of the occupied part of the single-particle spectral function. The latter can, in principle, be determined from angle-resolved photoemission (ARPES) data. As a consequence, the energy gain driving the development of the superconducting state is intimately related to the dramatic changes in the photoemission line shape when going below  $T_c$ . These points are illustrated in the context of the ‘‘mode’’ model used to fit ARPES data in the normal and superconducting states, where the question of kinetic-energy versus potential-energy-driven superconductivity is explored in detail. We use our findings to comment on the relation of ARPES data to the condensation energy and to various other experimental data. In particular, our results suggest that the nature of the superconducting transition is strongly related to how anomalous (non-Fermi-liquid-like) the normal-state spectral function is and, as such, is dependent upon the doping level.

## I. INTRODUCTION

The origin of high-temperature superconductivity in the cuprates is still a matter of great debate. Recently, there have been several different theoretical proposals for the mechanism of high- $T_c$  superconductivity, each of which leads to a characteristically different reason for the lowering of the free energy. This has focused attention on how various spectroscopic probes can yield information on the source of the condensation energy which drives the formation of the superconducting ground state.

The first, and perhaps the most radical, proposal is the interlayer tunneling theory of Anderson and co-workers, where it is conjectured that the condensation energy is due to a gain in the  $c$ -axis kinetic energy in the superconducting state.<sup>1</sup> Some measurements of the  $c$ -axis penetration depth<sup>2</sup> are in conflict with the predictions of this theory. Others, such as recent  $c$ -axis optical conductivity data<sup>3</sup> indicating a violation of the optical sum rule, are in support of this hypothesis, although alternative explanations have been proposed for these observations.<sup>4</sup> An even more unusual suggestion has been recently made by Hirsch and Marsiglio,<sup>5</sup> where they argue that the bulk of the condensation energy comes from a gain in the in-plane kinetic energy. A rather different approach proposes the lowering of the Coulomb energy in the long-wavelength, infrared region,<sup>6</sup> which has not been experimentally tested as yet. A fourth approach advocates a lowering of the exchange energy in the superconducting state due to the formation of a resonant mode in the dynamic spin

susceptibility<sup>7,8</sup> near  $\mathbf{q} = (\pi, \pi, \pi)$ , and has recently received experimental support from neutron scattering studies.<sup>9</sup>

We note that all of the above proposals focus on a part of the Hamiltonian describing the system: either a part of the kinetic energy or a part of the interaction energy. Correspondingly, the experiments to test these ideas focus on two-particle correlation functions in a specific region of momentum and frequency space.

In this paper we propose to exploit a very general exact relation between the one-particle Green's function of a system and its internal energy [see Eq. (1) below]. This approach, in principle, allows us to determine the ‘‘source’’ of the condensation energy *without* making any *a priori* assumptions about which piece of the Hamiltonian is responsible for the gain in condensation energy. The exact expression used involves moments of the occupied part of the one-electron spectral function, and since this quantity is directly related<sup>10</sup> to angle-resolved photoemission spectroscopy (ARPES) measurements, our approach also appears very promising from a practical point of view.

As a specific illustration of this general framework, we study the condensation energy for a very simple self-energy for the normal and superconducting states which captures the essential features of the observed ARPES line shapes, the so-called mode model.<sup>11–13</sup> This analysis leads to several interesting conclusions as discussed below, but most importantly, it suggests an intimate connection between the nature of the normal-state spectral function (Fermi liquid or non-Fermi liquid), the formation of sharply defined quasiparticle

excitations below  $T_c$ , and the gain in free energy in the superconducting state.

This paper is organized as follows. In Sec. II, the formalism relating the condensation energy to the spectral function is developed. In Sec. III, the mode model is introduced, and the nature of the resulting condensation energy is discussed. In Sec. IV, our observations concerning ARPES spectra are used to comment on the results of previous spectroscopic studies, as well as the origin of the condensation energy. In Sec. V, we address the question of the nature of the superconducting transition versus hole doping. In Sec. VI, we offer some concluding remarks. Finally, we include two appendices. Appendix A further explores questions raised in Sec. II in regards to the full Hamiltonian and the virial theorem. In Appendix B, we comment on the applicability of the formalism of Sec. II to experimental data (ARPES and tunneling).

## II. FORMALISM

We begin with the assumption that the condensation energy does not have a component due to phonons, though, as we mention below, this condition can be relaxed. We note that at optimal doping, the isotope exponent  $\alpha$  is essentially zero,<sup>14</sup> and Chester<sup>15</sup> proved that the change in ion kinetic energy between superconducting and normal states vanishes for  $\alpha=0$ . To proceed, we assume an effective single-band Hamiltonian which involves only two-particle interactions (possible limitations of this assumption will be discussed below). Then, simply exploiting standard formulas<sup>16,17</sup> for the internal energy  $U = \langle H - \mu N \rangle$  ( $\mu$  is the chemical potential and  $N$  the number of particles) in terms of the one-particle Green's function, we obtain

$$U_N - U_S = \sum_{\mathbf{k}} \int_{-\infty}^{+\infty} d\omega (\omega + \epsilon_k) f(\omega) [A_N(\mathbf{k}, \omega) - A_S(\mathbf{k}, \omega)], \quad (1)$$

where the spin variable has been summed over. Here and below the subscript  $N$  stands for the normal state,  $S$  for the superconducting state.  $A(\mathbf{k}, \omega)$  is the single-particle spectral function,  $f(\omega)$  the Fermi function, and  $\epsilon_k$  the bare energy dispersion which defines the kinetic energy part of the Hamiltonian. Note that the  $\mu N$  term has been absorbed into  $\omega$  and  $\epsilon_k$ ; that is, these quantities are defined relative to the appropriate chemical potential  $\mu_N$  or  $\mu_S$ . In general,  $\mu_N$  and  $\mu_S$  will be different. This difference has to be taken into account, since the condensation energy is small.

The condensation energy is defined by the zero-temperature limit of  $U_N - U_S$  in the above expression. Note that this involves defining (or somehow extrapolating to) the normal-state spectral function at  $T=0$ . Such an extrapolation, which we return to below, is not specific to our approach, but required in all estimates of the condensation energy. We remark that Eq. (1) yields the correct condensation energy  $N(0)\Delta^2/2$  for the BCS theory of superconductivity.<sup>18</sup>

We also note that Eq. (1) can also be broken up into two pieces to individually yield the thermal expectation value of the kinetic energy [using  $2\epsilon_k$  in the parentheses in front of  $f(\omega)$ ], and that of the potential energy (using  $\omega - \epsilon_k$  instead). Further, this expression can also be generalized to the

free energy by including the entropy term as discussed by Wada.<sup>19</sup> Moreover, if the phonons can be treated in a harmonic approximation, the terms missing in Eq. (1) (half the electron-phonon interaction and all other phonon terms) reduce to twice the phonon kinetic energy.<sup>17,19</sup> The phonon kinetic energy can then be determined if the isotope coefficient is known.<sup>15</sup> For  $\alpha=1/2$ , the missing terms in this approximation reduce to twice the condensation energy, so that Eq. (1) is realized again, but with a *negative* sign.

The great advantage of Eq. (1) is that it involves just the occupied part of the single-particle spectral function, which is measured by angle-resolved photoemission spectroscopy.<sup>10</sup> Therefore, in principle, one should be able to derive the condensation energy from such data, if an appropriate extrapolation of the normal-state spectral function to  $T=0$  can be made. On the other hand, a disadvantage is that the bare energies  $\epsilon_k$  are *a priori* unknown. Note that these are not directly obtained from the measured ARPES dispersion, which already includes many-body renormalizations; nor are they simply determined by the eigenvalues of a band calculation, as such calculations also include an effective potential term. Rather, they could be determined by projecting the kinetic energy operator onto the single-band subspace. Methodologies for doing this when reducing to an effective single-band Hubbard model have been worked out for the cuprates<sup>20</sup> and could be exploited for this purpose.

Equation (1) trivially reduces to the following:

$$U_N - U_S = \sum_{\mathbf{k}} \epsilon_k [n_N(\mathbf{k}) - n_S(\mathbf{k})] + \int_{-\infty}^{+\infty} d\omega \omega f(\omega) [N_N(\omega) - N_S(\omega)], \quad (2)$$

where  $n(\mathbf{k})$  is the momentum distribution function and  $N(\omega)$  the single-particle density of states. While ARPES has the advantage of giving information on both terms in this expression, other techniques could be exploited as well for the individual terms in Eq. (2). For instance,  $n(\mathbf{k})$  in principle can be obtained from positron annihilation or Compton scattering, while  $N(\omega)$  could be determined from tunneling data, although matrix elements could be a major complication for both tunneling and ARPES.

We conclude this section with some remarks about a low-energy effective single-band Hamiltonian used to derive Eq. (1) versus the *full* Hamiltonian of the solid which includes quadratic dispersions for all (valence and core) electrons and ionic kinetic energies, together with all Coulombic interactions (see, e.g., Ref. 15). As shown by Chester<sup>15</sup> the full  $H$  can be very useful for studying the condensation energy. We discuss some points related to such a description in Appendix A.

Here we only wish to emphasize one important point which will come up later in our analysis. In terms of the full Hamiltonian, the transition to the superconducting state must be driven by a gain in the potential energy (ignoring ion terms for this argument), as is intuitively obvious and also rigorously shown by Chester using the virial theorem. However, the kinetic energy terms in the effective single-band Hamiltonian can (and in general do) incorporate effects of the potential energy terms of the full Hamiltonian. Further,

there is no virial theorem restriction on the expectation values of the kinetic and potential terms of the effective Hamiltonian (since these do not, in general, obey the requisite homogeneity conditions). As a consequence, there is nothing preventing the effective low-energy Hamiltonian from having a superconducting transition driven by a lowering of the (effective) kinetic energy.

### III. MODE MODEL

To illustrate the power of the formalism, as well as some of the subtleties discussed above, we now analyze the condensation energy arising from a spectral function described by a simple model self-energy which captures some of the essential features of the ARPES data in the important region of the Brillouin zone near  $(\pi,0)$  in the cuprates. These features are (1) a broad normal-state spectral function  $A$  which seems  $T$  independent in the normal state (except in the underdoped case, where there is a pseudogap which fills in as  $T$  increases), and thus can be used as the extrapolated “normal” state  $A_N$  down to  $T=0$  in Eq. (1); (2) a superconducting-state spectral function  $A_S$  which shows a gap, a sharp quasiparticle peak, and a dip-hump structure at higher energies. At a later stage, we will have to make some reasonable assumptions about the  $\mathbf{k}$  dependence of the spectral functions to perform the zone sum in Eq. (1).

These nontrivial changes in the ARPES line shape going from the normal to the superconducting state have been attributed<sup>11,12</sup> to the interaction of an electron with an electronic resonant mode below  $T_c$ , which itself arises self-consistently from the line shape change. Strong arguments have been given which identify this resonant mode with one observed by magnetic neutron scattering.<sup>11,13</sup> Thus our analysis below will also have bearing upon the arguments mentioned in the Introduction which relate the resonant mode directly to changes in the exchange energy.

The simplest version of the resonant mode model is a self-energy of the form

$$\Sigma = \frac{\Gamma}{\pi} \ln \left| \frac{\omega - \omega_0 - \Delta}{\omega + \omega_0 + \Delta} \right| + i\Gamma \Theta(|\omega| - \omega_0 - \Delta), \quad (3)$$

where  $\omega_0$  is the resonant-mode energy,  $\Delta$  the superconducting energy gap, and  $\Theta$  the step function. (A more complicated form has been presented in earlier work.<sup>12</sup>) This self-energy is then used in the superconducting state spectral function<sup>18</sup>

$$A = \frac{1}{\pi} \text{Im} \frac{Z\omega + \epsilon}{Z^2(\omega^2 - \Delta^2) - \epsilon^2}, \quad (4)$$

where  $Z=1-\Sigma/\omega$ . We note that for this form of  $\Sigma$ , the spectral function  $A_S$  will consist of two  $\delta$  functions located at  $\pm E$ , where  $E$  satisfies two conditions: (1) it has a value less than  $\omega_0 + \Delta$  and (2) the denominator of Eq. (4) vanishes. The weight of the  $\delta$  functions is then determined as<sup>22</sup>  $|dA^{-1}(\pm E)/d\omega|$ . In addition, there are incoherent pieces for  $|\omega|$  greater than  $\omega_0 + \Delta$ . We use the same self-energy for the (extrapolated) normal state with  $\Delta=0$  and  $\omega_0=0$ , so that  $A_N$  reduces to a Lorentzian centered at  $\epsilon$  with a full width at half maximum of  $2\Gamma$ .

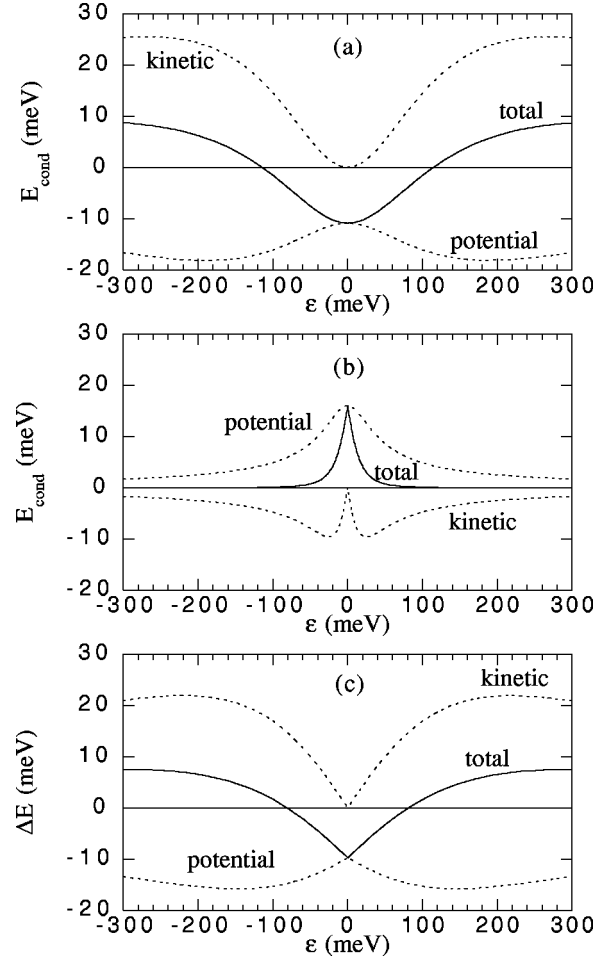


FIG. 1. (a) Condensation energy contribution  $E_{cond}$  vs single-particle energy  $\epsilon$  for the model self-energy of Eq. (3). As discussed in the text, the quantity plotted is the result (as a function of  $\epsilon$ ) after the  $\omega$  integration is done in Eq. (1). The parameters are  $\Gamma=230$  meV,  $\Delta=32$  meV, and  $\omega_0=41.6$  meV, which were obtained from fits to ARPES spectra at  $(\pi,0)$  (Ref. 12). The normal state is obtained by setting  $\omega_0$  and  $\Delta$  to zero. The dotted lines are a decomposition of  $E_{cond}$  into separate kinetic and potential energy pieces. (b) Condensation energy contribution for the BCS theory using the same  $\Delta$ . (c) A repeat of (a), but with the superconducting state replaced by the normal state with  $\omega_0=41.6$  meV (and so labeled as  $\Delta E$  instead of  $E_{cond}$ ).

To begin with, for simplicity, we treat both  $\omega_0$  and  $\Delta$  as momentum independent. It is straightforward to evaluate Eq. (1) with the sum over momentum reducing to an integral over  $\epsilon$ . In Fig. 1(a), we plot the integrand of the  $\epsilon$  integral (i.e., after the  $\omega$  integral has been done). The parameters used are the same ones used earlier<sup>12</sup> to fit ARPES data near optimal doping at the  $(\pi,0)$  point. The result is somewhat surprising. The integrand is negative for  $\epsilon$  near zero (i.e.,  $k$  near  $k_F$ ) and positive for  $\epsilon$  far enough away. This should be contrasted with the BCS result,<sup>23</sup> shown in Fig. 1(b), where the contribution at  $k_F$  (which is  $\Delta/2$ ) is maximal and positive.

To gain insight into this unusual result, we also show in Fig. 1(a) the decomposition of this result into kinetic and potential energy pieces. Unlike BCS theory [Fig. 1(b)], where the condensation is driven by the potential energy, in the mode model case, it is kinetic energy driven. To under-

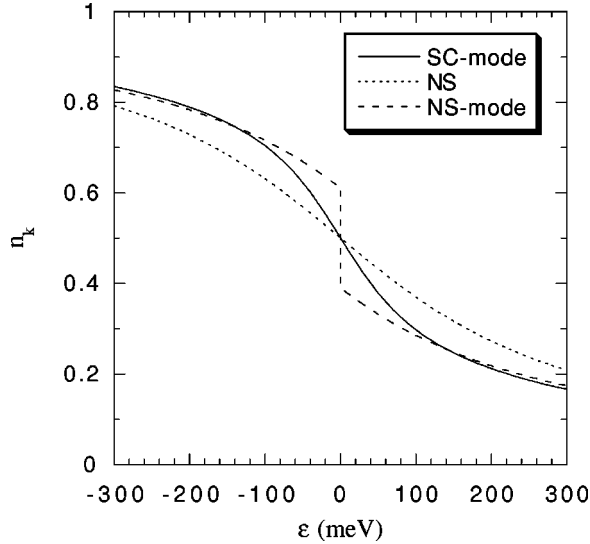


FIG. 2. Momentum distribution function vs  $\epsilon$  in the superconducting state (SC), normal state with  $\omega_0=0$  (NS), and in the normal state with  $\omega_0=41.6$  meV (NS mode). Same parameters as Fig. 1.

stand the unusual decrease in the kinetic energy as one goes below  $T_c$ , we show in Fig. 2 the momentum distribution function  $n(\mathbf{k})$  plotted versus  $\epsilon$ . Note that in contrast to BCS theory,  $n(\mathbf{k})$  is *sharper* in the superconducting state than in the normal state. The reason is very simple. The (extrapolated) normal state is subject to a large broadening  $\Gamma$  all the way down to  $T=0$  which smears out  $n(\mathbf{k})$  on the scale of  $\Gamma$ . At  $T=0$  the result is simply  $n_N(\mathbf{k})=1/2-\tan^{-1}(\epsilon/\Gamma)/\pi$ . In the superconducting state, although  $\Delta$  broadens  $n(\mathbf{k})$  as in BCS theory, one now has quasiparticle peaks. The effect of this on sharpening  $n(\mathbf{k})$  is much larger than the broadening due to  $\Delta$  (for  $\Delta \ll \Gamma$ ), so the net effect is a significant sharpening. As a consequence, the kinetic energy is lowered in the superconducting state.

Note that these counterintuitive results would not have been obtained had  $\omega_0$  retained the same (nonzero) value in the normal state. In this case, sharp quasiparticles would exist in the normal state, and all of our usual expectations are fulfilled:  $n_N(\mathbf{k})$  would have had a step discontinuity (also illustrated in Fig. 2), and the normal-state kinetic energy would have been considerably lower than the superconducting one. In fact, for this situation, the model is equivalent to that of Einstein phonons in an approximation where the gap is treated as a (real) constant in frequency.<sup>18</sup> However, the normal-state ARPES data near  $(\pi,0)$  are clearly consistent with  $\omega_0=0$  and are  $T$  independent with a  $\Gamma \gg T$ , which suggests that the  $T=0$  extrapolation used here is reasonable.

These points are further illustrated in Fig. 1(c), where we show the energy difference between the normal state with  $\omega_0$  nonzero and the normal state with  $\omega_0$  zero. Note the similarity to Fig. 1(a); i.e., the unusual behavior in Fig. 1(a) is due to the formation of a gap in the incoherent part of the spectral function, with the resulting appearance of quasiparticle states, and thus not simply due to the presence of a superconducting energy gap  $\Delta$ . Now, in the real system, it is the transition to a phase-coherent superconducting state which leads to the appearance of the resonant mode at nonzero energy, which causes the gap in  $\text{Im}\Sigma$ , which results in the incoherent gap and quasiparticles, which in turn generates

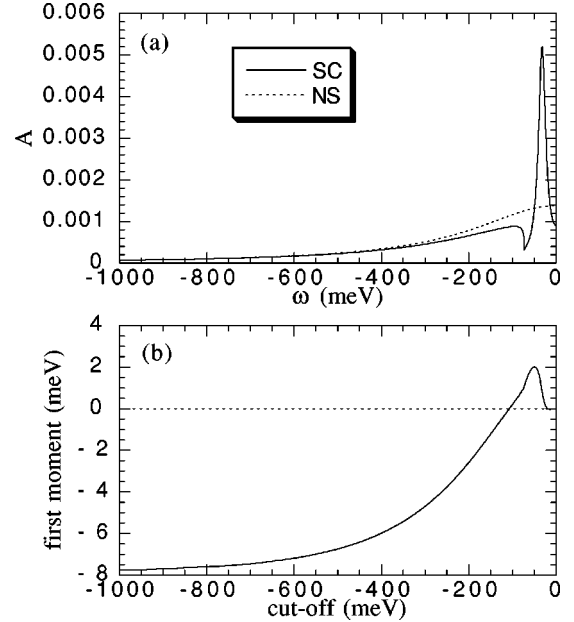


FIG. 3. (a) Spectral function at the Fermi surface ( $\epsilon=0$ ) in the superconducting (SC) and normal states (NS). (b) First moment contribution of (a) to the condensation energy vs the lower cutoff in the  $\omega$  integration in Eq. (1). Note the positive contribution of the quasiparticle peak and the large negative contribution from the high-energy tail. Same parameters as Fig. 1.

the mode. Although this self-consistency loop clearly indicates the electron-electron nature of the interaction (as opposed to an electron-phonon one), the connection of these effects with the onset of phase coherence (as opposed to the opening of a spectral gap, which is known to occur at a higher temperature  $T^*$ ) is not understood at this time. That is, the mode model is a crude simulation of the consequences of some underlying microscopic theory which has yet to be developed.

As for the potential energy piece, we note that the contribution to Eq. (1) at  $k_F$  (where  $\epsilon_k=0$ ) reduces to the first moment of the spectral function. In Fig. 3(a), we plot the spectral function at  $k_F$  in both the normal and superconducting states. (For illustrative purposes, we have replaced the  $\delta$  function peaks in the superconducting state by Lorentzians of half width at half maximum 10 meV). From this plot, we note that the quasiparticle peaks give a positive contribution to the condensation energy, but that at higher energies (large  $|\omega|$ ), there is a negative contribution. This negative contribution is very important because it is weighted by  $\omega$  in the integrand of Eq. (1). To see this quantitatively, we plot in Fig. 3(b) the first moment difference at the Fermi surface ( $\epsilon_k=0$ ) as a function of the lower cutoff on the  $\omega$  integration (the upper cutoff at  $T=0$  is  $\omega=0$ ). We clearly see the positive contribution due to the quasiparticle peak and the (5 times larger) negative contribution due to the incoherent tail. This explains why the net contribution from the potential energy term is negative. We can contrast this with BCS theory, where only the quasiparticle part exists, and so the net contribution is positive.

An interesting question concerns what happens in this model as the broadening  $\Gamma$  is reduced. In Fig. 4, we show results as for Fig. 1(a), but for various  $\Gamma$  values. As  $\Gamma$  is



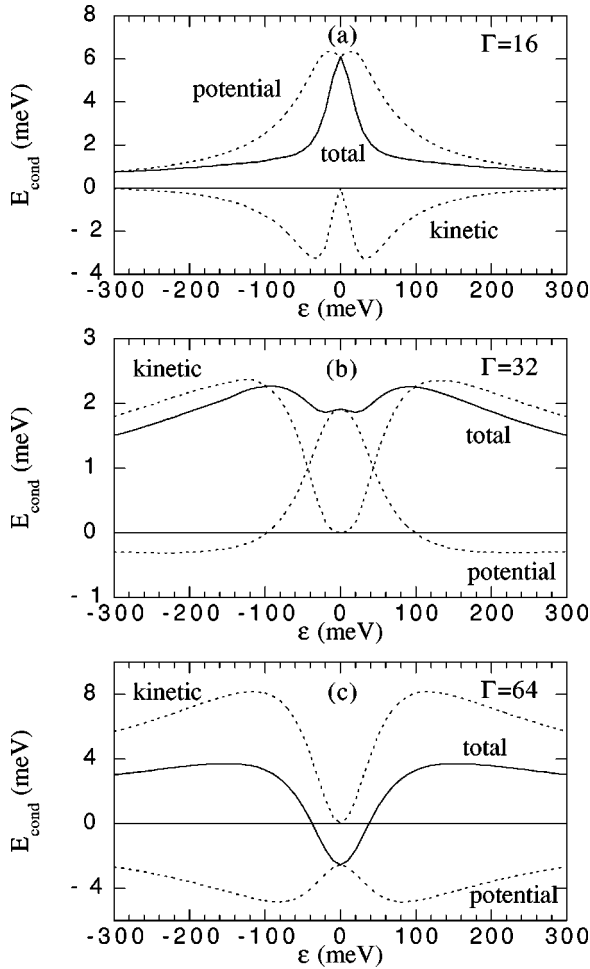


FIG. 4. Condensation energy contribution, as in Fig. 1(a), for (a)  $\Gamma=16$  meV, (b) 32 meV, and (c) 64 meV. Here  $\Delta$  and  $\omega_0$  are both 32 meV. Note the crossover from kinetic-energy-driven behavior to potential-energy-driven behavior as  $\Gamma$  is reduced.

reduced and becomes comparable to  $\Delta$ , one crosses over from the unusual behavior in Fig. 1(a) to a behavior very similar to that of BCS theory in Fig. 1(b). That is, the condensation energy crosses over from being kinetic energy driven to being potential energy driven. This is not a surprise, since in the limit that  $\Gamma$  goes to zero, the model reduces to BCS theory. The physics behind this, though, is quite interesting. For large  $\Gamma$ , the normal state is very non-Fermi-liquid-like. As  $\Gamma$  is reduced, though, the normal state becomes more Fermi-liquid-like.<sup>24</sup> As a consequence, one crosses over from being kinetic energy driven to potential energy driven (when  $\Gamma \sim \Delta$ ). The relation of kinetic energy driven behavior with the presence of a non-Fermi-liquid normal state and a Fermi liquid superconducting state was realized early on by Anderson<sup>25,1</sup> and will be returned to again in Sec. IV. Figure 4 also draws attention to the fact that being kinetic or potential energy driven is a relative point. Note in Fig. 4(b) that near  $k_F$ , the two contributions have the *same* sign. Individual terms, such as the potential energy in Fig. 4(b) and the kinetic energy in other cases we have explored, can even change sign as a function of  $\epsilon_k$ .

A noteworthy feature of the above calculations is the large contribution in Figs. 1 and 4 at large  $|\epsilon|$ . In particular, in most cases, the bulk of the contribution to the condensa-

tion energy comes well away from the Fermi surface, in contrast to BCS theory. In Fig. 1(a), this is due to the large  $\Gamma$ , which leads to a substantial rearrangement of the spectral function even for large  $|\epsilon|$ , causing large contributions to both the potential and kinetic energy pieces. Even in the case of Fig. 4(a), where  $\Gamma$  is quite small, there is still a potential energy contribution at large  $|\epsilon|$ . This can be traced to the gap in the incoherent part of the spectral function, with the resulting spectral weight being recovered around  $\omega = \epsilon$ , leading to a potential energy shift. Even in the BCS case, Fig. 1(b), the individual potential and kinetic energy pieces would not converge if integrated over an infinite range in  $\epsilon$ . In BCS theory, this is corrected by an ultraviolet cutoff (the Debye frequency). We elect not to include such a cutoff in the mode model, since it would lead to another adjustable parameter, and the  $\epsilon$  integral is bound by the band edges, and so is convergent. In the real system, the ‘‘mode’’ effects in the spectral function disappear as one approaches the band edges, and as discussed in the following paragraph, this effect can be crudely simulated by setting the mode energy proportional to  $\Delta_k$ , the latter quantity in the  $d$ -wave case vanishing along the zone diagonal where the band edges are located.

Although we plot only the differences in Figs. 1, 3(b), and 4, the individual normal- and superconducting-state terms are quite large. This raises the question of what the value of Eq. (1) would actually be if summed over the zone. To do this, we must make some assumptions about what the momentum dependence of various quantities is. For simplicity sake, we will treat  $\Gamma$  as  $k$  independent, though we note that available ARPES data are consistent with this quantity being reduced in size as one moves from  $(\pi, 0)$  towards the Fermi crossing along the  $(\pi, \pi)$  direction. In the first sum, denoted by case (a), we treat  $\Delta$  and  $\omega_0$  as  $k$  independent. In the second sum, denoted by case (b), we replace  $\Delta$  by  $\Delta_k = \Delta_0[\cos(k_x a) - \cos(k_y a)]/2$ , where  $\Delta_k$  is the standard  $d$ -wave gap function, but still retain a  $k$ -independent  $\omega_0$ . In the third sum (c), in addition to the  $d$ -wave  $\Delta_k$  we also take  $\omega_0 = c|\Delta_k|$ , with the  $k$  dependence of  $\omega_0$  crudely simulating the fact that the mode effects in the spectral function are reduced as one moves away from the  $(\pi, 0)$  points of the zone.<sup>12</sup> The values of these parameters are the same as used in Fig. 1(a), and are consistent with ARPES and neutron data for Bi2212 ( $\Gamma = 230$  meV,  $\Delta_0 = 32$  meV,  $c = 1.3$ ). To perform the zone sum, we have to make some assumptions on what the  $\epsilon_k$  are. As the mode model is designed to account for the difference between the normal state and superconducting state, we elect to use normal state ARPES dispersions for  $\epsilon_k$ ,<sup>26</sup> though we caution that this represents a different choice for the ‘‘kinetic’’ energy part of the effective single-band Hamiltonian than is typically used.<sup>27</sup> Because this dispersion has particle-hole asymmetry, the chemical potential will not be the same in the superconducting state as in the normal state. The chemical potential is thus tuned to achieve the same density (a hole doping  $x = 0.16$ ) as the normal state. Note that the normal state density itself is a function of  $\Gamma$  (we assume  $\omega_0 = 0$  for the normal state).

Performing the zone sum, we find condensation energies of +3.6, +3.3, and +1.1 meV, per CuO plane, for cases (a), (b), and (c), respectively. We note that the last result is the more physically appropriate, and though small, is somewhat

larger than the condensation energy of 1/4 meV per plane estimated by Loram *et al.* from specific heat data for optimal doped  $\text{YBa}_2\text{Cu}_3\text{O}_7$  (YBCO).<sup>28</sup> The above values will be reduced if a more realistic  $k, \omega$  dependence is used for  $\Gamma$ , since, as we noted above,  $\Gamma$  decreases as one moves away from  $(\pi, 0)$ . As consistent with Fig. 1(a), the contribution to the condensation energy is negative for an anisotropic shell around the Fermi surface (due to the anisotropy of  $\Delta_k$  and  $\epsilon_k$ ) and positive outside of this shell. Again, this will be sensitive to the  $k$  dependence of  $\Gamma$ , as can be seen from Fig. 4. We also remark that there are chemical potential shifts of +2.6, +2.1, and +1.4 meV, respectively, for cases (a), (b), and (c). Again, the last value is the more physically appropriate. It is very interesting to note that somewhat smaller positive shifts (around +0.6 meV) have been seen experimentally in YBCO.<sup>29</sup> These shifts are a consequence of particle-hole asymmetry and the change in  $n_k$  when going into the superconducting state.

#### IV. CONNECTIONS WITH PREVIOUS WORK

While a quantitative evaluation of Eq. (1) using experimental data as input on the right hand side must await further progress as discussed in Appendix B, several qualitative points can be made even at this stage. From Eq. (1), there is a one to one correspondence between the changes in the spectral function and the condensation energy. That is, the condensation energy is due to the profound change in line shape seen in photoemission data when going below  $T_c$ . When summed over the zone, this in turn leads to changes in the tunneling density of states [second part of Eq. (2)]. These spectral function changes cause, and are themselves caused by, changes of various two particle correlation functions, such as the optical conductivity and the dynamic spin susceptibility, which have previously been used by others to comment about the nature of the condensation energy.

In this context, we now discuss the earlier work concerning the  $c$ -axis conductivity. The most dramatic changes in the ARPES line shape when going below  $T_c$  occur near the  $(\pi, 0)$  points of the zone. It is exactly these points of the zone which appear to have the largest  $c$ -axis tunneling matrix elements associated with them.<sup>31</sup> Previous work has found a strong correlation between the  $c$ -axis conductivity and ARPES spectra near the  $(\pi, 0)$  points of the zone.<sup>32,4</sup> Therefore, it is rather straightforward to speculate that it is the formation of strong quasiparticle peaks in these regions of the zone and the resulting changes in the spectral function at higher binding energy, which are responsible for the lowering of the  $c$ -axis kinetic energy. We note that earlier, Anderson<sup>25,1</sup> had remarked that if the quasiparticle weight is coming from high binding energy, then one would expect a lowering of the kinetic energy. This in fact is what is occurring in the mode model calculations, though we note from our work that the true quantity which determines the sign of the kinetic energy change in the vicinity of  $k_F$  is the gradient of the momentum distribution function at  $k_F$ .

We also remark that the change in  $c$ -axis kinetic energy has been recently addressed by Ioffe and Millis in the context of the same mode model used in the current paper.<sup>4</sup> These effects would enter directly in Eq. (1) by including a  $c$ -axis tunneling contribution to  $\epsilon_k$ .<sup>4</sup> As for the in-plane kinetic

energy, it is so large that it is difficult to determine its contribution to Eq. (1) from optical conductivity data because of some of the same normalization concerns mentioned in Appendix B in regards to ARPES and tunneling data. Still, if the mode model calculation is a reflection of reality, we can speculate that  $n(\mathbf{k})$  will probably sharpen in the superconducting state, leading to a lowering of the in-plane kinetic energy. How large the effect will be is somewhat difficult to determine, in that the same regions of the zone where large changes are seen in the ARPES line shape are also characterized by small Fermi velocities (the optical conductivity involves a zone sum weighted by  $v_F^2$ ). Along the  $(\pi, \pi)$  direction, for instance, there is still some controversy concerning how dramatic the line shape change is below  $T_c$ .<sup>33,34</sup> Also, as can be seen from Fig. 4, this question is very dependent on the variation of the normal state line shape in the zone. Although the line shape near  $(\pi, 0)$  is highly non-Fermi-liquid-like, the behavior along the  $(\pi, \pi)$  direction appears to be marginal Fermi-liquid-like.<sup>33,34</sup> As remarked in Sec. III, the more Fermi-liquid-like the normal state line shape is, the greater the tendency is to switch over to potential energy driven behavior instead. Improved experimentation should again lead to a resolution of these issues.

This brings us to the question concerning the relation of the magnetic resonant mode observed by neutron scattering to the condensation energy. All calculations of the resonant mode assume the existence of quasiparticle peaks. In the absence of such quasiparticle peaks, a sharp resonance is not expected. That is, the sharp resonance observed by neutron scattering and the resulting lowering in the exchange energy part of the  $t$ - $J$  Hamiltonian are again a consequence of the formation of quasiparticle states. In this context, it is important to note that the  $d$ -wave coherence factors associated with quasiparticle states are important for the formation of the resonance, whether in the context of calculations in the particle-hole channel<sup>35</sup> or in the particle-particle scenario proposed by Demler and Zhang.<sup>36</sup> In any case, this again supports our statement, motivated by Eq. (1), that it is the dramatic change in the ARPES spectra below  $T_c$  which is the source of the condensation energy.

In this regard, we note a puzzling feature in connection with the mode model. Although it was designed to take into account the effect of the magnetic resonance mode on the spectral function, the condensation in the mode model is kinetic energy driven. This is in contrast to the potential-energy-driven nature of the condensation with the resonant mode discussed in the context of the  $t$ - $J$  model,<sup>7-9</sup> despite the same underlying physics. There are two possibilities for this apparent discrepancy. First, the breakup of the Hamiltonian into potential and kinetic energy pieces depends on the particular single-band reduction which is done. The superexchange energy, which is a kinetic energy effect at the level of the Hubbard model,<sup>30</sup> appears as a potential energy term when reduced to the  $t$ - $J$  Hamiltonian. In the mode model, the kinetic energy is equated to  $\epsilon_k$  based on normal-state ARPES dispersions,<sup>27</sup> while the potential energy term leads to effects described by the  $\Sigma$  of Eq. (3).

The second possibility is that the argument of Ref. 8 is confined to low energies of order  $\Delta$ . As demonstrated in Fig. 3(b), if the mode model is confined to such energy scales, the first moment (i.e., the potential) term would reverse sign,

since the quasiparticle peak always gives a positive contribution to the first moment. That is, one would expect the resonance to lower the exchange energy since it is a consequence of the quasiparticle states, which lower the potential energy in Eq. (1). It is the difference in the high-energy incoherent tails (Fig. 3), though, which is ultimately responsible for the increase of the net potential energy in Fig. 1(a). This would imply that the neutron scattering results<sup>9</sup> may change if more complete data at higher energies and other  $q$  values are obtained. That is, the true answer will depend on where the weight for the neutron resonance is coming from, in complete analogy to the earlier mentioned argument of Anderson<sup>25</sup> in regards to where the quasiparticle weight is coming from.

This discussion again emphasizes that the current debate concerning kinetic-energy-driven superconductivity versus potential-energy-driven superconductivity must be kept in proper context, as the very definition of the kinetic and potential pieces is dependent upon what effective low-energy Hamiltonian one employs and what energy range one considers.

## V. DOPING DEPENDENCE

The condensation energy as estimated from specific heat is known to decrease strongly as the doping is reduced.<sup>28</sup> This is despite the increase of the spectral gap.<sup>37,38,13</sup> There are two reasons for this suggested by the above line of reasoning. First, the normal state itself at  $T_c$  already exhibits a large spectral gap, the so-called pseudogap, which acts to reduce the difference in Eq. (1). Second, the weight of the quasiparticle peak strongly decreases as the doping is reduced.<sup>13</sup> This reduces the quasiparticle contribution to both the first moment and to  $n(\mathbf{k})$ . We caution that the normal-state extrapolation down to  $T=0$  will be more difficult to estimate for underdoped experimental data because of the influence of the pseudogap, which is known to fill in as a function of temperature.<sup>39</sup> Still, the available underdoped ARPES and tunneling data are certainly in support of a smaller condensation energy than overdoped data due to the pseudogap, which is in agreement with conclusions based on specific heat data.<sup>40</sup> The new contribution to these arguments is the strong reduction of the weight of the quasiparticle peak in the underdoped case which makes the condensation energy smaller still. In fact, based on our arguments, the strong reduction of the superfluid density upon underdoping is almost certainly connected with the strong reduction in the quasiparticle weight.

Finally, Anderson<sup>41</sup> has speculated that the superconducting transition temperature is potential energy driven on the overdoped side and kinetic energy driven on the underdoped side. This is a distinct possibility, since  $\Gamma$  is known from ARPES data<sup>33</sup> to be strongly reduced as the doping increases on the overdoped side, and as Fig. 4 demonstrates, one might expect (if the mode model is a reflection of reality) a crossover from kinetic-energy-driven behavior to potential-energy-driven behavior as  $\Gamma$  is reduced. In this context, we note the result of Basov *et al*<sup>3</sup> that the lowering of the  $c$ -axis kinetic energy appears to be confined to the underdoped side of the phase diagram. Moreover, if one attributes  $T^*$  on the underdoped side to the onset of pairing correlations,<sup>42</sup> then

one anticipates a potential energy gain due to pairing to occur at this finite temperature crossover. At  $T_c$ , phase coherence in the pair field is established, and the resulting quasiparticle formation<sup>43</sup> and related spectral changes could lead to a kinetic-energy-driven transition of the sort discussed above. We emphasize “could,” since in the context of Eq. (1), there is no unambiguous evidence yet from real ARPES data that such is the case.

## VI. CONCLUDING REMARKS

We conclude this paper by noting that the above arguments based on condensation energy considerations highlights one of the key question of the high- $T_c$  problem: why do quasiparticle peaks only appear below  $T_c$ ? This is especially relevant in the underdoped case, since the spectral gap turns on at a considerably higher temperature than  $T_c$ , but the quasiparticle peaks again form only at  $T_c$ .<sup>43</sup> This implies that there is a deep connection between the onset of phase coherence in the pair field and the onset of coherence in the single electron degrees of freedom.<sup>1</sup> We suggest that the understanding of this connection will be central to solving the high- $T_c$  problem. The result of the current paper is that Eq. (1) brings this issue into much sharper focus. In particular, as a cautionary note, the incoherent part of the spectral function is likely to be as important as the quasiparticle component in determining the condensation energy (Fig. 3). That is, it is the overall shape of the spectral function [the peak-dip-hump behavior of Fig. 3(a)], rather than just the quasiparticle part, which is ultimately responsible for the total condensation energy. We believe that experimental data analyzed in the context of Eq. (1) will play an important role in providing a solution to the high- $T_c$  problem.

## ACKNOWLEDGMENTS

We thank Hong Ding, Helen Fretwell, Adam Kaminski, and Joel Mesot for discussions concerning the ARPES data, and Laura Greene, Christophe Renner, and John Zasadzinski for providing their tunneling data. This work was supported by the the U.S. Department of Energy, Basic Energy Sciences, under Contract No. W-31-109-ENG-38, National Science Foundation Contract No. DMR 9624048, and Contract No. DMR 91-20000 through the Science and Technology Center for Superconductivity. M.R. was supported in part by the Indian DST through the Swarnajayanti scheme.

## APPENDIX A: THE FULL HAMILTONIAN AND THE VIRIAL THEOREM

In this appendix, we make further comments on some issues which were briefly discussed at the end of Sec. II, relating to the use of the full Hamiltonian versus an effective single-band Hamiltonian.

We note that as written, Eq. (1) does not apply to the *full* Hamiltonian of the solid which includes all the electronic and ionic degrees of freedom together with their Coulombic interactions as discussed in Ref. 15. In principle an expression similar to Eq. (1) could be written if the quantities in Eq. (1) were replaced by matrices in reciprocal lattice space.<sup>44</sup> For our purposes, where an energy difference is being looked at, a unitary transformation to band index space



would be desirable. The resulting off-diagonal terms would then represent interband transitions. These could be of potential importance, even for the energy difference. For example, the violation of the  $c$ -axis optical conductivity sum rule<sup>3</sup> implies a change in interband terms so that the total optical sum rule is satisfied.

The usefulness of the full Hamiltonian is that one can use the virial theorem<sup>15,21</sup>  $2K - nV - 3P\Omega = 0$ , exploiting the fact that the kinetic energy  $K$  is a homogeneous function of order 2 in momentum, and the potential energy  $V$  is a homogeneous function of order  $n$  in position. Here  $P$  is the pressure and  $\Omega$  denotes the volume. For Coulomb forces  $n = -1$ , and ignoring the pressure terms (which are negligible at ambient pressure), this reduces to  $2K + V = 0$ .

If we assume that the form of Eq. (1) applies to the full Hamiltonian (which could be possible if all interband terms dropped out of the energy difference, as well as all electron-ion and ion-ion terms), then by using the virial theorem, the right hand side of Eq. (2) can be shown to reduce to  $2/3$  the first moment of the density of states at  $T=0$ . In addition, the change in the kinetic energy would be the negative of the condensation energy, with the potential energy twice the condensation energy.

This reduced form of Eq. (2), though, must be treated with extreme caution, and is likely not useful to the problem at hand. The reason is that the kinetic energy and potential energy terms of the full Hamiltonian are not the same as the kinetic and potential energy terms of the effective single-band Hamiltonian. It is only for the former that the virial theorem manipulations would be allowed. As an example, BCS theory obeys Eq. (2), but not the reduced form.

## APPENDIX B: COMMENTS ON ARPES AND TUNNELING

The purpose of Sec. III was to demonstrate how Eq. (1) works out in practice for a model where exact calculations could be done. This is important when considering real experimental data. We have spent considerable effort analyzing Eqs. (1) and (2) using experimental data from ARPES and tunneling as input, and plan to report on these endeavors in a future publication. But given what we have learned from the mode model, some of the problems associated with an analysis based on experimental data can be appreciated. First, the condensation energy is obtained by subtracting two large numbers. Therefore, normalization of the data becomes a central concern. Problems in this regard when considering

$n(\mathbf{k})$ , which is the zeroth moment of the ARPES data, were discussed in a previous experimental paper.<sup>45</sup> For the first moment, these problems are further amplified due to the  $\omega$  weighting in the integrand. This can be appreciated from Fig. 3, where the bulk of the contribution in the mode model comes from the mismatch in the high-energy tails of the normal-state and superconducting-state spectral functions. When analyzing real data, we have found that the tail contribution, either from ARPES or from tunneling, is very sensitive to how the data are normalized. Different choices of normalization can even lead to changes in sign of the first moment.

Another concern concerns the  $\mathbf{k}$  sum in Eq. (1). Both ARPES and tunneling have (their own distinct)  $\mathbf{k}$ -dependent matrix elements, which lead to weighting factors not present in Eq. (1). For ARPES, these effects can in principle be factored out by either theoretical estimates of the matrix elements<sup>46</sup> or by comparing data at different photon energies to obtain information on them.<sup>47</sup> For tunneling, information on matrix elements can be obtained by comparing different types of tunneling [scanning tunnel microscopy (STM), tunnel junction, point contact] or by employing directional tunneling methods.

Another issue in connection with experimental data is an appropriate extrapolation of the normal state to zero temperature. Information on this can be obtained by analyzing the temperature dependence of the normal-state data, remembering that the Fermi function will cause a temperature dependence of the data which should be factored out before attempting the  $T=0$  extrapolation. We finally note that the temperature dependence issue is strongly coupled to the normalization problem mentioned above. In ARPES, the absolute intensity can change due to temperature-dependent changes in absorbed gases, surface doping level, and sample location.<sup>45</sup> In tunneling, the absolute conductance can change due to temperature-dependent changes in junction characteristics. In both cases, changes of background emission with temperature is another potential problem.

Despite these concerns, we believe that with careful experimentation, many of these difficulties can be overcome, and even if an exact determination of Eq. (1) is not possible, insights into the origin of the condensation energy will certainly be forthcoming from the data. This is particularly true for ARPES, which has the advantage of being  $\mathbf{k}$  resolved and thus giving one information on the relative contribution of different  $\mathbf{k}$  vectors to the condensation energy.

<sup>1</sup>P. W. Anderson, *The Theory of Superconductivity in the High- $T_c$  Cuprates* (Princeton University Press, Princeton, 1997).

<sup>2</sup>K. A. Moler, J. R. Kirtley, D. G. Hinks, T. W. Li, and M. Xu, *Science* **279**, 1193 (1998); A. A. Tsvetkov, D. van der Marel, K. A. Moler, J. R. Kirtley, J. L. de Boer, A. Meetsma, Z. F. Ren, N. Kolesnikov, D. Dulic, A. Damascelli, M. Gruninger, J. Schutzmann, J. W. van der Eb, H. S. Somal, and J. H. Wang, *Nature* (London) **395**, 360 (1998).

<sup>3</sup>D. N. Basov, S. I. Woods, A. S. Katz, E. J. Singley, R. C. Dynes, M. Xu, D. G. Hinks, C. C. Homes, and M. Strongin, *Science* **283**, 49 (1999).

<sup>4</sup>L. B. Ioffe and A. J. Millis, *Science* **285**, 1241 (1999); *Phys. Rev. B* **61**, 9077 (2000).

<sup>5</sup>J. E. Hirsch and F. Marsiglio, cond-mat/9908322 (unpublished).

<sup>6</sup>A. J. Leggett, *J. Phys. Chem. Solids* **59**, 1729 (1998); *Phys. Rev. Lett.* **83**, 392 (1999).

<sup>7</sup>D. J. Scalapino and S. R. White, *Phys. Rev. B* **58**, 8222 (1998).

<sup>8</sup>E. Demler and S.-C. Zhang, *Nature* (London) **396**, 733 (1998).

<sup>9</sup>P. Dai, H. A. Mook, S. M. Hayden, G. Aeppli, T. G. Perring, R. D. Hunt, and F. Dogan, *Science* **284**, 1344 (1999).

<sup>10</sup>M. Randeria, H. Ding, J. C. Campuzano, A. Bellman, G. Jennings, T. Yokoya, T. Takahashi, H. Katayama-Yoshida, T. Mo-



- chiku, and K. Kadowaki, *Phys. Rev. Lett.* **74**, 4951 (1995).
- <sup>11</sup>M. R. Norman, H. Ding, J. C. Campuzano, T. Takeuchi, M. Randeria, T. Yokoya, T. Takahashi, T. Mochiku, and K. Kadowaki, *Phys. Rev. Lett.* **79**, 3506 (1997).
- <sup>12</sup>M. R. Norman and H. Ding, *Phys. Rev. B* **57**, R11 089 (1998).
- <sup>13</sup>J. C. Campuzano, H. Ding, M. R. Norman, H. M. Fretwell, M. Randeria, A. Kaminski, J. Mesot, T. Takeuchi, T. Sato, T. Yokoya, T. Takahashi, T. Mochiku, K. Kadowaki, P. Guptasarma, D. G. Hinks, Z. Konstantinovic, Z. Z. Li, and H. Raffy, *Phys. Rev. Lett.* **83**, 3709 (1999).
- <sup>14</sup>J. Franck, in *Models and Phenomenology for Conventional and High-Temperature Superconductivity*, edited by G. Iadonisi, J. R. Schrieffer, and M. L. Chiofalo (IOS Press, Amsterdam, 1998), p. 269.
- <sup>15</sup>G. V. Chester, *Phys. Rev.* **103**, 1693 (1956).
- <sup>16</sup>L. P. Kadanoff and G. Baym, *Quantum Statistical Mechanics* (W. A. Benjamin, New York, 1962), Chap. 2; A. L. Fetter and J. D. Walecka, *Quantum Theory of Many-Particle Systems* (McGraw-Hill, New York, 1971), Chap. 7.
- <sup>17</sup>D. J. Scalapino and J. R. Schrieffer, *Proceedings of the Eastern Theoretical Physics Conference* (University of North Carolina, Chapel Hill, 1963), Vol. 1, p. 2; D. J. Scalapino, in *Superconductivity*, edited by R. D. Parks (Marcel Dekker, New York, 1969), Vol. 1, p. 449.
- <sup>18</sup>J. R. Schrieffer, *Theory of Superconductivity* (W. A. Benjamin, New York, 1964).
- <sup>19</sup>Y. Wada, *Phys. Rev.* **135**, A1481 (1964).
- <sup>20</sup>A. K. McMahan, R. M. Martin, and S. Satpathy, *Phys. Rev. B* **38**, 6650 (1988); M. S. Hybertsen, M. Schluter, and N. E. Christensen, *ibid.* **39**, 9028 (1989).
- <sup>21</sup>L. D. Landau and E. M. Lifshitz, *Statistical Physics* (Pergamon, London, 1958), p. 92.
- <sup>22</sup>G. D. Mahan, *Many-Particle Physics* (Plenum, New York, 1990), p. 157.
- <sup>23</sup>M. Tinkham, *Introduction to Superconductivity* (McGraw-Hill, New York, 1975).
- <sup>24</sup>For the purposes of this paper, by a Fermi liquid, we mean a quasiparticle peak which is sharp compared to its energy position. We note that the normal state  $\text{Im } \Sigma$  in the mode model is a constant, and thus does not vanish as  $\omega^2$ .
- <sup>25</sup>P. W. Anderson, *Phys. Rev. B* **42**, 2624 (1990).
- <sup>26</sup>M. R. Norman, M. Randeria, H. Ding, and J. C. Campuzano, *Phys. Rev. B* **52**, 615 (1995).
- <sup>27</sup>In the mode model, the normal state self-energy is an imaginary constant, so the normal-state dispersion reduces to that from the effective kinetic energy term. This would not be true in a more sophisticated model which had a frequency-dependent self-energy.
- <sup>28</sup>J. W. Loram, K. A. Mirza, and P. F. Freeman, *Physica C* **171**, 243 (1990).
- <sup>29</sup>G. Rietveld, N. Y. Chen, and D. van der Marel, *Phys. Rev. Lett.* **69**, 2578 (1992).
- <sup>30</sup>P. W. Anderson, *Adv. Phys.* **46**, 3 (1997).
- <sup>31</sup>S. Chakravarty, A. Sudbo, P. W. Anderson, and S. Strong, *Science* **261**, 337 (1993); O. K. Andersen, A. I. Liechtenstein, O. Jepsen, and F. Paulsen, *J. Phys. Chem. Solids* **56**, 1573 (1995).
- <sup>32</sup>C. Bernhard, D. Munzar, A. Wittlin, W. Konig, A. Golnik, C. T. Lin, M. Klaser, Th. Wolf, G. Muller-Vogt, and M. Cardona, *Phys. Rev. B* **59**, R6631 (1999).
- <sup>33</sup>A. Kaminski, J. Mesot, H. Fretwell, J. C. Campuzano, M. R. Norman, M. Randeria, H. Ding, T. Sato, T. Takahashi, T. Mochiku, K. Kadowaki, and H. Hoechst, *Phys. Rev. Lett.* **84**, 1788 (2000).
- <sup>34</sup>T. Valla, A. V. Fedorov, P. D. Johnson, B. O. Wells, S. L. Hulbert, Q. Li, G. D. Gu, and N. Koshizuka, *Science* **285**, 2110 (1999).
- <sup>35</sup>P. Monthoux and D. J. Scalapino, *Phys. Rev. Lett.* **72**, 1874 (1994); H. F. Fong, B. Keimer, P. W. Anderson, D. Reznik, F. Dogan, and I. A. Aksay, *ibid.* **75**, 316 (1995).
- <sup>36</sup>E. Demler and S.-C. Zhang, *Phys. Rev. Lett.* **75**, 4126 (1995).
- <sup>37</sup>J. M. Harris, Z.-X. Shen, P. J. White, D. S. Marshall, M. C. Schabel, J. N. Eckstein, and I. Bozovic, *Phys. Rev. B* **54**, 15 665 (1996).
- <sup>38</sup>N. Miyakawa, J. J. Zasadzinski, L. Ozyuzer, P. Guptasarma, D. G. Hinks, C. Kendziora, and K. E. Gray, *Phys. Rev. Lett.* **83**, 1018 (1999).
- <sup>39</sup>M. R. Norman, H. Ding, M. Randeria, J. C. Campuzano, T. Yokoya, T. Takeuchi, T. Takahashi, T. Mochiku, K. Kadowaki, P. Guptasarma, and D. G. Hinks, *Nature (London)* **392**, 157 (1998).
- <sup>40</sup>J. W. Loram, K. A. Mirza, J. R. Cooper, W. Y. Liang, and J. M. Wade, *J. Supercond.* **7**, 243 (1994).
- <sup>41</sup>P. W. Anderson (private communication).
- <sup>42</sup>For a review, see M. Randeria, in *Models and Phenomenology for Conventional and High-Temperature Superconductivity*, edited by G. Iadonisi, J. R. Schrieffer, and M. L. Chiofalo (IOS Press, Amsterdam, 1998), p. 53.
- <sup>43</sup>M. R. Norman, M. Randeria, H. Ding, and J. C. Campuzano, *Phys. Rev. B* **57**, R11 093 (1998).
- <sup>44</sup>L. Hedin and S. Lundqvist, *Solid State Phys.* **23**, 1 (1969).
- <sup>45</sup>J. C. Campuzano, H. Ding, H. Fretwell, J. Mesot, A. Kaminski, T. Sato, T. Takahashi, T. Mochiku, and K. Kadowaki, cond-mat/9811349 (unpublished).
- <sup>46</sup>A. Bansil and M. Lindroos, *Phys. Rev. Lett.* **83**, 5154 (1999).
- <sup>47</sup>J. Mesot, A. Kaminski, H. M. Fretwell, M. Randeria, J. C. Campuzano, H. Ding, M. R. Norman, T. Takeuchi, T. Sato, T. Yokoya, T. Takahashi, I. Chong, T. Terashima, M. Takano, T. Mochiku, and K. Kadowaki, cond-mat/9910430 (unpublished).